

*Article*

## Seismic Shear Strengthening of Reinforced Concrete Short Columns Using Ferrocement with Expanded Metal

Songkran Panyamul<sup>1,a</sup>, Phaiboon Panyakap<sup>1,b,\*</sup>, and Anat Ruangrassamee<sup>2</sup>

<sup>1</sup> Department of Civil Engineering and Urban Development, School of Engineering, Sripatum University, Bangkok 10900, Thailand

<sup>2</sup> Department of Civil Engineering, Faculty of Engineering, Chulalongkorn University, Bangkok 10330, Thailand

E-mail: <sup>a</sup>songkranpan9@gmail.com, <sup>b</sup>phaiboon.pa@spu.ac.th (Corresponding author)

**Abstract.** Typical reinforced concrete short column is brittle in shear rather than flexure under lateral cyclic loading due to its shear deficiency. This paper presents the improvement of seismic behaviour of the reinforced concrete short columns which were strengthened by using ferrocement with expanded metal. Full scale experiments were conducted for two strengthened concrete columns with different volume fractions of expanded metal and the control specimen under lateral cyclic loading. It was found that the seismic behaviour in terms of the shear strength, stiffness, displacement ductility, and energy dissipation were significantly improved. The expanded metal mesh with the high specific surface provided the better performance for controlling the crack propagation. The brittle shear failure mode of the stirrup was reduced and the ductile flexure mode of the longitudinal reinforcement was dominant. The reduced shear force of the stirrup was compensated by the shear force of the expanded metal reinforcement which experienced relatively large strain. The technique of steel angle installation at the corners of column can successfully prevent the effect of sharpened corner wrapping of the mesh. A model to predict the shear strength of the strengthened column is presented in term of the global efficiency factor for expanded metal.

**Keywords:** Shear strengthening, reinforced concrete, short columns, ferrocement, expanded metal.

**ENGINEERING JOURNAL** Volume 23 Issue 6

Received 24 May 2019

Accepted 22 August 2019

Published 30 November 2019

Online at <http://www.engj.org/>

DOI:10.4186/ej.2019.23.6.175

## 1. Introduction

Experience from the 2014 Mae Lao earthquake in the northern part of Thailand showed that many existing reinforced concrete buildings were damaged due to the brittle shear failure of columns [1]. This is due to the insufficient stirrup reinforcement of the existing columns, particularly for short columns. Typically, the presence of partial infilled wall leads to shorten the height of column resulting in an increase of the lateral force under earthquake load. Therefore, shear strengthening of the short columns is required for seismic retrofit. Among several methods of seismic strengthening, ferrocement is well-known as a satisfactory alternative due to its ease for application and reasonable cost. However, seismic performance of reinforced concrete column confined with ferrocement is dependent on several factors. Takiguchi and Abdullah [2] investigated the effects of volume fraction of wire mesh reinforcement by using different layers of wire mesh. The specimen with four layers of wire mesh provided the effective shear strength of column. The number of layers of wire mesh required to strengthen the columns with circular jacketing was proposed. In addition, the similar equation to predict the shear strength of square RC columns confined with square ferrocement jacket was also proposed [3]. Similar retrofit columns were also conducted [4], six specimens with four circular jacket and two square jacket were tested under lateral cyclic loading. It was found that significant ductility of the strengthened column was achieved for both types of jacketing. Kazemi and Morshed [5] studied the shear strength of short reinforced concrete columns retrofitted with expanded steel mesh using the volume fraction of 0.008, 0.016 and 0.024. The shear strength and ductility of the retrofit columns were significantly enhanced in comparison with the original columns. The ductility capacity was also improved with the increase of volume fraction, however, the shear strength could not be investigated because the quantities of stirrup reinforcement of the tested specimens could not be comparable. On the other hand, stainless steel wire mesh with permeable polymer concrete mortar was also employed as ferrocement to retrofit the circular RC column [6]. The columns were jacketed at various heights in the plastic hinge region. It was found that retrofitting with stainless steel wire mesh in the plastic hinge region could enhance the flexural strength and ductility of circular RC columns. Further investigation of the repaired circular RC columns by using stainless steel wire mesh jacket was also conducted [7]. The repaired columns showed a low rate of stiffness degradation. Furthermore, the repaired specimens provided significant improvement on the shear strength, ductility and energy dissipation capacity.

The earlier studies on the use of expanded metal mesh [8, 9] reported that expanded metal mesh provide approximately equal strength when compared with welded-wire mesh. But, the expanded metal mesh is stiffer than the wire mesh that tends to minimize crack width which leads to the better impact resistance and crack control. However, the lack of flexibility for the thick gages causes the difficulty in wrapping especially for the sharp curves except for cut strips. In structural application, ACI 549.1R [10] suggested that expanded metal meshes must be considered for the orientation of mesh by using the global efficiency factors of reinforcement recommended for a member subjected to uniaxial tension or bending. Recent study [11] also reported that the orientation, the size of the cells, and the number of cells affected the yielding resistance of expanded metal panel. In addition, the flattened expanded metal panel sustained higher strength than the standard expanded metal panel [12]. However, there is no information on the global efficiency factors when apply to shear design because the lack of available test data on the shear capacity of ferrocement.

To overcome the effect of sharp curves, especially for the retrofit of rectangular column, several researchers [13-15] proposed the rounded corner technique to reduce the stress concentration at the corners of rectangular column. Kaish [16-18] investigated three techniques of square ferrocement jacketing, i.e., square jacketing with rounded corner column, square jacketing with shear keys at the center of each face of column, square jacketing with extra layer mesh at each corner of column. The results showed that the rounded corner column provided the best load capacity in eccentric load case. The extra layer mesh column is the best for concentric load case.

The effect of shear bond between concrete and ferrocement was also studied. Li [19, 20] observed that ferrocement was delaminated from concrete in the strengthening of reinforced concrete beam-column joint using ferrocement jacket. To maintain the bonding between concrete and ferrocement, Li and Lam [21] investigated four types of shear keys for ferrocement and concrete, i.e., M6 expansive anchors, M6 and M8 adhesive anchors, and L-shape anchors. It was found that the adhesive shear keys are better than the expansive shear keys. Among various types of shear keys, the L-shape adhesive anchors are the most effective shear keys including that a roughened surface for concrete is also recommended.

In this study, the strengthening technique for short reinforced concrete columns is proposed by using ferrocement with expanded metal meshes. Full scale experiments were conducted for the two strengthened concrete columns and the control specimen under lateral cyclic loading. In the strengthening process, the technique of steel angle installation at the corner of column was employed to avoid the effect of sharpened corner wrapping of the mesh. The confinement of steel angle was to protect against corner cracking of column due to the stress concentration of sharpened corner wrapping. In addition, this technique is suitable for the thick gages expanded metal mesh which is rather difficult to wrap the column. Strain gauge measurements were installed to investigate the seismic behaviour of column.

## 2. Experimental Program

### 2.1. Materials Properties

The expanded metal in this study is the standard type steel meshes with overlapped rhomb-shape stitches diamond shape mesh pattern. The steel mesh type 1 and type 2 according to JIS G3351 [22] were selected for the reinforcement of the ferrocement. The rhomb-shape and the physical properties of expanded metal are shown in Fig. 1 and Table 1, respectively. The steel bar of each mesh has the yield strength, the ultimate strength and the elastic modulus of 337 MPa, 400 MPa and 135 GPa, respectively [23, 24]. The steel mesh in the longitudinal direction (L) of the diamond is stronger than the perpendicular short direction (S) in which the expansion took place. In the application of wrapping on the column for strengthening, the longitudinal direction (L) of the diamond mesh should be placed in the horizontal direction parallel to the applied lateral force.

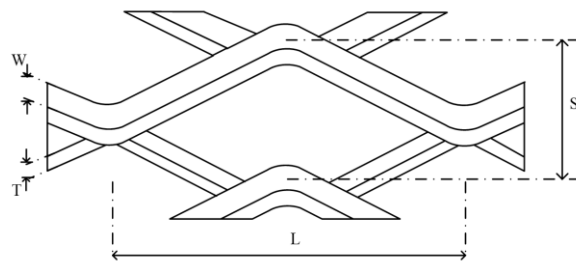


Fig. 1. Expanded Metal shape.

Table 1. Properties of Expanded Metal.

| Expanded Metal | S<br>(mm) | L<br>(mm) | T<br>(mm) | W<br>(mm) | Weight<br>(kg/m <sup>2</sup> ) |
|----------------|-----------|-----------|-----------|-----------|--------------------------------|
| Type 1         | 12.0      | 30.5      | 2.3       | 3.0       | 5.25                           |
| Type 2         | 34.0      | 76.2      | 2.3       | 5.0       | 9.39                           |

The plastered mortar of ferrocement has the proportion of cement to sand ratio of 1:2, and water to cement ratio of 0.45. The mortar specimen has the 28 days compressive strength of 22.25 MPa which was tested according to ASTM C349 [25].

### 2.2. Test Specimens

Three reinforced concrete columns C0, C1, C2 with a cross section of 0.40×0.40 m and a height of 1.10 m were prepared for laboratory testing. The longitudinal reinforcements were twenty four of 25 mm diameter deformed steel bars with symmetrical arrangement at each side of column. The stirrup reinforcements were 6 mm diameter round bar at a spacing of 200 mm. To investigate the shear strength of column, the strength of the control specimen should be governed by shear rather than flexure. Therefore, the high percentage of the longitudinal reinforcement is to protect the flexural failure of the column. The cylindrical compressive strength of concrete was 35 MPa at 28 days. The deformed bar and the round bar have the yield strength of 400 MPa and 240 MPa, respectively, and both steel bars have the elastic modulus of 210

GPa. The C0 column was represented for the control specimen, as shown in Fig. 2a. The C1 and C2 columns were strengthened by the ferrocement with the type 1 and type 2 expanded metals, respectively, as shown in Fig. 2b.

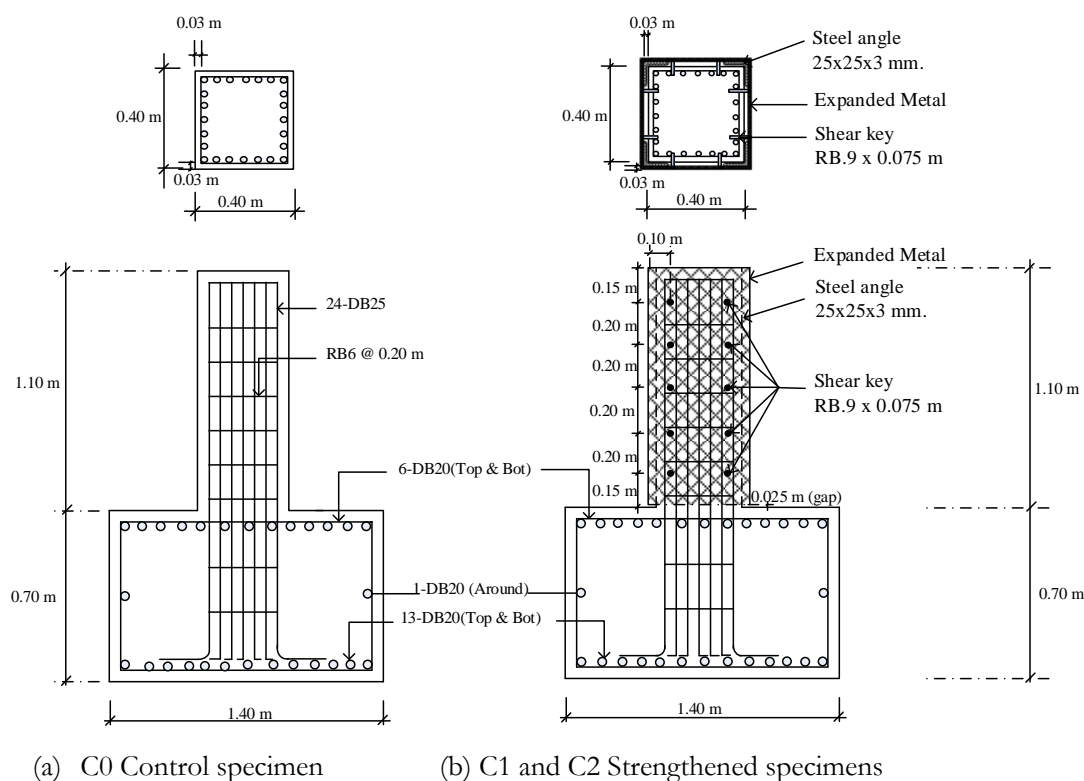


Fig. 2. Control and strengthened specimens.

In the strengthening process, four 25×25 mm steel angles were installed at each corner of columns. The expanded metal sheets were cut into four strips and they were laminated at each side of columns. The vertical edges of each expanded metal strip were welded to the steel angle by the welding electrode. Two 9 mm diameter steel tie rods were employed as adhesive shear keys at an embedded depth of 75 mm and a spacing of 200 mm along the height of columns. The tie rods were round bars with the yield strength of 240 MPa, and they were fixed to the concrete with the non-shrink grouting. The use of steel angle was to reduce the effect of stress concentration at the corners of rectangular columns. The adhesive tie rod shear keys were provided to prevent bond failure of the ferrocement. The ferrocement jacket was 30 mm thickness through the height of columns, except that a gap of 25 mm was provided at the column base to avoid the increase of flexural capacity of ferrocement. The volume fraction ( $V_f$ ) of reinforcement in the ferrocement for the C1 and C2 were 0.022 and 0.039 respectively, where  $V_f$  is the total volume of reinforcement divided by the volume of ferrocement composite. The specific surface ( $S_f$ ) of reinforcement in the ferrocement for the C1 and C2 were 0.0294  $m^{-1}$  and 0.0186  $m^{-1}$  respectively, where  $S_f$  is the total bonded area of reinforcement divided by the volume of ferrocement composite. The reinforcement details of the test specimens C0, C1, C2 are shown in Table 2. The preparation of reinforcement of the strengthened specimens is presented in Fig. 3.

Table 2. Reinforcement details of the test specimens.

| Specimen | Ferrocement reinforcement | $V_f$ | $S_f(m^{-1})$ | Longitudinal reinforcement | Stirrup reinforcement |
|----------|---------------------------|-------|---------------|----------------------------|-----------------------|
| C0       | -                         | -     | -             | 24DB25                     | RB6 @200              |
| C1       | Type 1 expanded metal     | 0.022 | 0.0294        | 24DB25                     | RB6 @200              |
| C2       | Type 2 expanded metal     | 0.039 | 0.0186        | 24DB25                     | RB6 @200              |



Fig. 3. Reinforcement of the strengthened specimens.

### 3. Test Setup and Loading System

The column specimen was supported by a concrete cube foundation overlaid on the strong concrete floor. The footing of the column specimen was anchored by a 32 mm diameter steel rebar at each side of the column through the concrete cube foundation and the strong concrete floor to prevent tilting under the applied lateral loading. The MTS 1500 kN hydraulic actuator was connected in the horizontal direction to the top of the specimen for applying the lateral load, as shown in Fig. 4. The top of specimen was attached to a 400 kN hydraulic jack for applying the vertical axial load which was maintained constant during the test. The horizontal hydraulic actuator was placed at 2.80 m height above the ground level. This specified elevation was to keep the shear span length ( $L_s = 0.70$  m) equal to twice of the depth of column (0.35 m). The shear span length is the distance between the column base and the edge of the bearing steel plate of the MTS actuator that applied the lateral load. The horizontal displacements at the top of the specimen including vertical and rotational displacements of the columns were recorded by using strain-type displacement transducers.

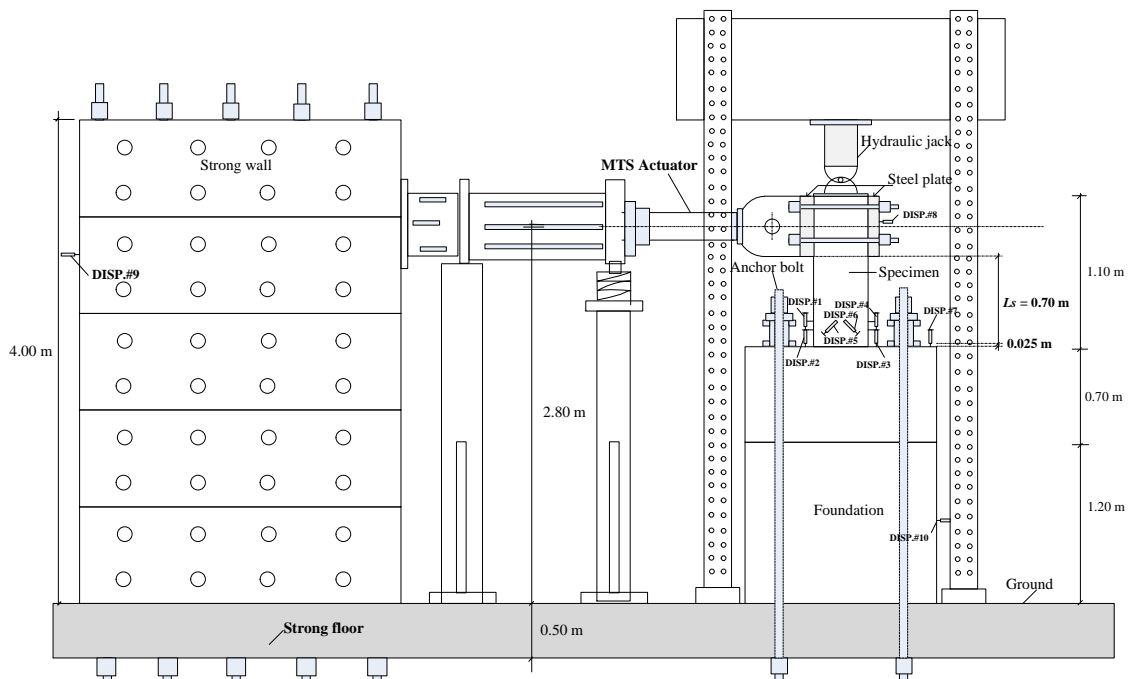


Fig. 4. Test setup of the experimental specimen.

To investigate the seismic behaviour of column, four pairs of strain gauges were attached to the longitudinal steel bars, i.e., 1-L, 1-R, 2-L, 2-R, 3-L, 3-R, 4-L, 4-R, where, L and R were represented for the

left and the right hand sides of the column, respectively. Two pairs of strain gauges were attached to the stirrup bars, i.e., ST1-F, ST1-B, ST2-F, ST2-B, where, ST stands for the stirrup, F and B are represented for the front and the back sides of the column, respectively. Two pairs of strain gauges were attached to the expanded metal bars, i.e., EXP1-F, EXP1-B, EXP2-F, EXP2-B, where, EXP stands for the expanded metal mesh. The installations of strain gauges of the experimental specimens are shown in Fig. 5.

The cyclic loading was performed under displacement control according to FEMA 461 [26] in steps of 0.1 % lateral drift up to 0.5%. After that the displacement was increased in steps of 0.25% until the lateral load carrying capacity of the specimen was less than 80% of the peak strength.

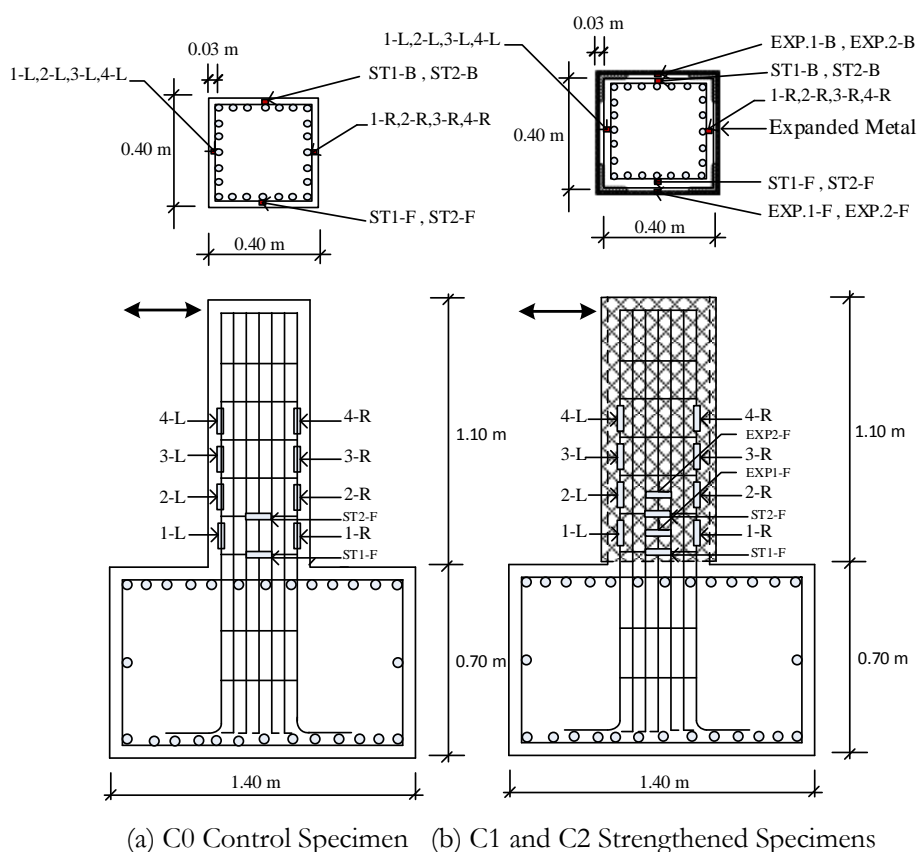


Fig. 5. Strain gauges of the experimental specimens.

## 4. Experimental Results

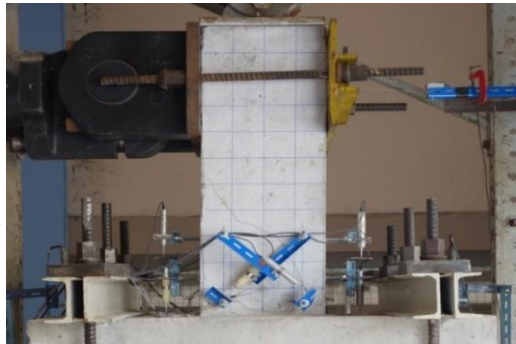
### 4.1. Failure of the Specimen C0

During the loading stage, the failure patterns of the specimen C0, which is the control specimen, at drift levels of 0.4%, 1.00 %, 2.00% are shown in Figs. 6a, 6b, 6c, respectively. The first diagonal crack was developed with an inclined angle about 45 degrees due to brittle shear failure at the drift level of 0.4%. The vertical length of crack was approximately equal to the depth of column. The crack width was enlarged and further propagated until the drift level of 2.00% at which the peak strength of column was reached. At the final stage, severe damage could be observed at both side of column due to the diagonal shear failure as shown in Fig. 6d.

### 4.2. Failure of the Specimen C1

The failure patterns of the specimen C1 at the drift levels of 0.75%, 2.0%, 3.25% are shown in Figs. 7a, 7b, 7c, respectively. The small crack started at the upper part of column due to the stress concentration of the loading stage of the actuator at the drift level of 0.75%. The crack propagated to the lower part of column

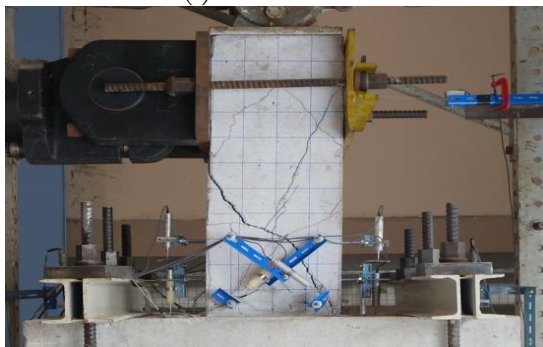
with the increase of drift level due to flexure-shear failure of concrete. However, the pattern of crack scattered throughout the column height until the peak strength was reached at the drift 3.25 %. The column strength was gradually degraded and followed by the spalling of ferrocement resulting in the exposure of the expanded metal mesh. Finally the column failed due to the widened flexure-shear crack of the column as shown in Fig. 7d. It was observed that the crack width of the specimen C1 was obviously smaller than that of the specimen C0.



(a) drift +0.4 %



(b) drift +1.00 %



(c) drift +2.00%



(d) Failure

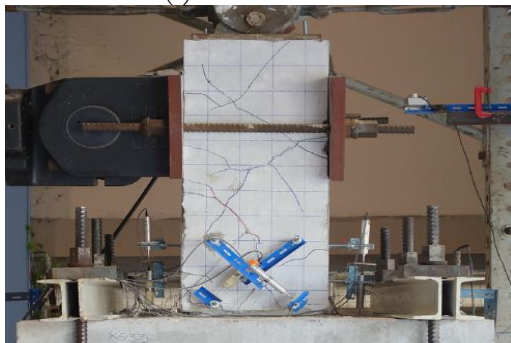
Fig. 6. Failure mechanisms of the specimen C0.



(a) drift +0.75 %



(b) drift +2.0 %



(c) drift +3.25



(d) Failure

Fig. 7. Failure mechanisms of specimen C1.

### 4.3. Failure of the Specimen C2

The failure patterns of the specimen C2 at the drift levels of 0.75%, 2.0%, 3.25% are shown in Figs. 8a, 8b, 8c, respectively. The crack patterns of the specimen C2 was similar to that of the specimen C1 when compared to each drift level. It was observed that slightly damage due to flexure-shear mode could be detected without diagonal shear crack at both sides of the column. However, due to the higher specific surface ( $S_v$ ) of reinforcement of the specimen C1 when compared to the specimen C2, the crack propagation of C1 was less than that of C2. As a result, the expanded metal mesh with the high specific surface provided the better performance for controlling the crack propagation. The specimen C2 could sustain the lateral load up to 4.00% drift at which the peak strength of the column was reached. The drift was larger than that of the specimen C1 due to the increase of the volume fraction of the expanded metal reinforcement of ferrocement. After the peak strength level, the spalling crack of ferrocement occurred due to the flexure-shear failure as shown in Fig. 8d. However, the damage of specimen C2 was less than that of C1 due to the increase of the volume fraction of the expanded metal that could enhance the shear strength of the column. Therefore, the seismic behaviour was dominated by flexure rather than shear. At the end of testing, the expanded metal meshes were still interlocked with the corners of the strengthened columns and they maintained their original shape without twisting. This indicated that the technique of steel angle installation at the corners of column can successfully prevent the effect of sharpened corner wrapping of the mesh.

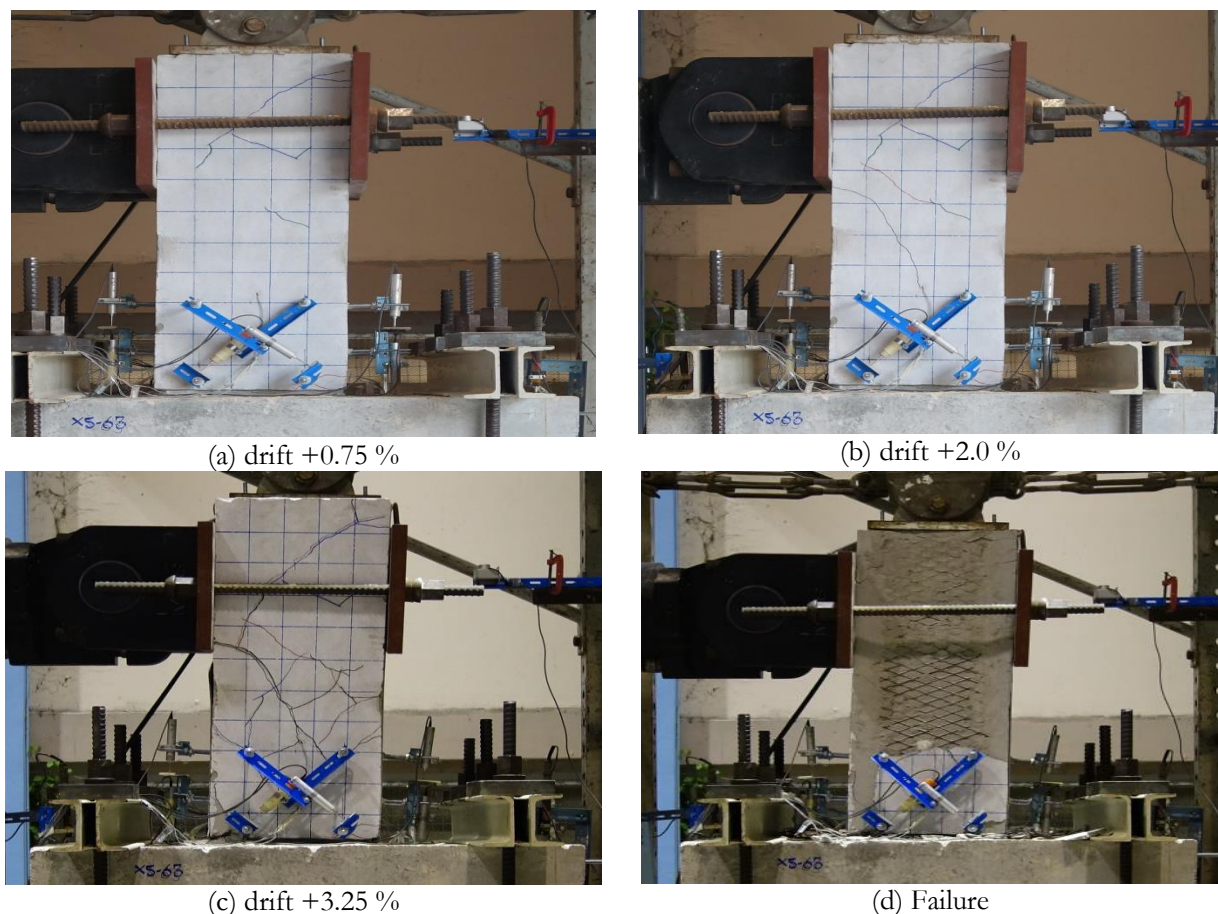


Fig. 8. Failure mechanisms of specimen C2.

### 4.4. Hysteretic Behaviour of the Specimens

The hysteretic behaviour in terms of the horizontal force-displacement relations of the specimens C0, C1 and C2 are shown in Figs. 9a, 9b and 9c, respectively. The enveloped curves of the three specimens are also presented in Fig. 9d. The strength and ductility of the strengthened specimens were significantly

improved when compared to that of the control specimen. In addition, the strengthened specimen C2 has greater stiffness and strength than the specimen C1 due to the increase of the volume fraction of the expanded metal reinforcement of ferrocement.

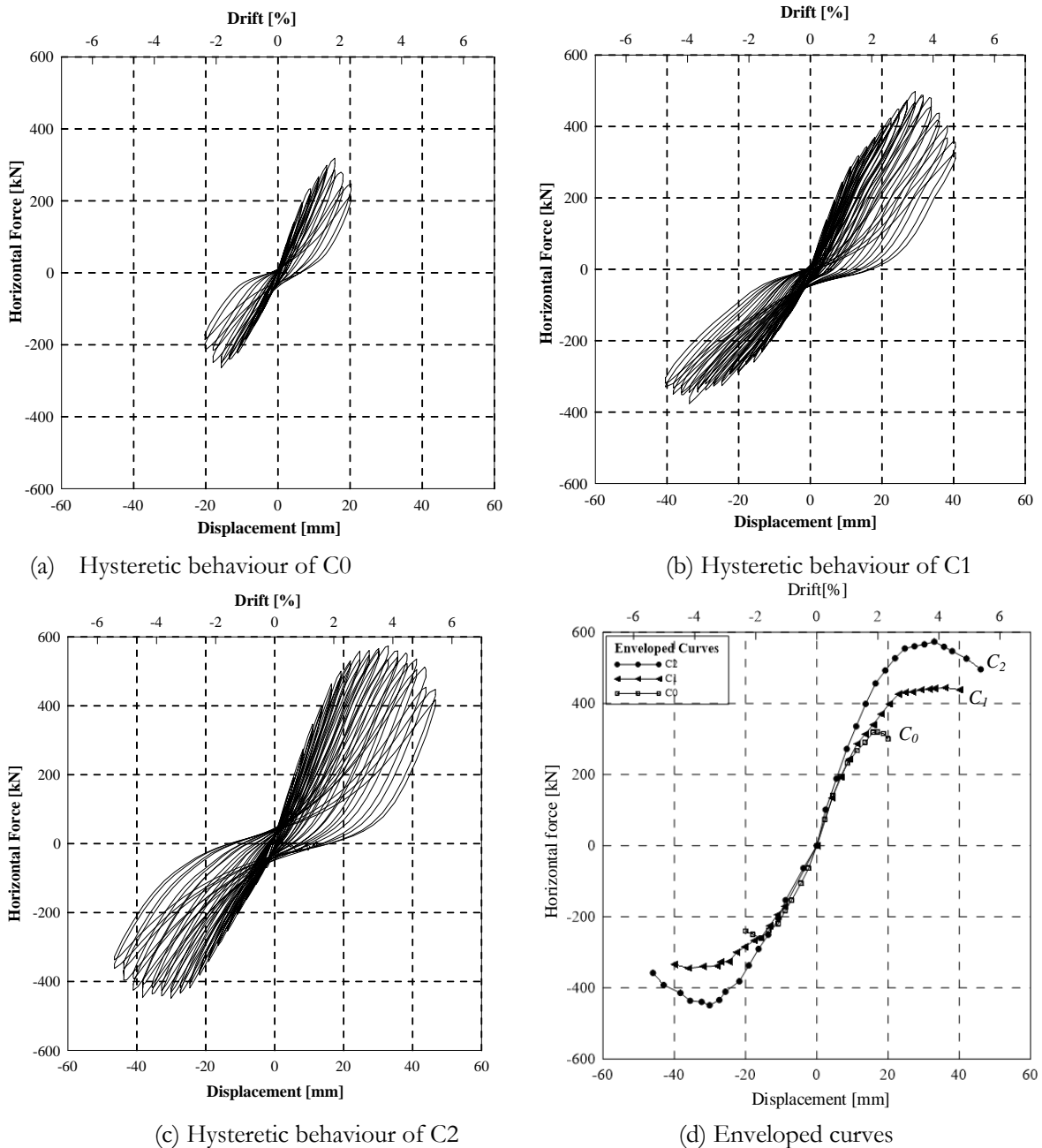


Fig. 9. Hysteretic behaviour of C0, C1 and C2.

The comparisons between the strength and displacement at the yield point of the three specimens are presented in Table 3. The test results reveal that the yield strength of the strengthened specimens C1 and C2 are 1.32 and 1.60 times that of the control specimen C0, respectively. Similarly, the peak strength of the strengthened specimens C1 and C2 are 1.55 and 1.79 times that of the control specimen C0, as shown in Table 4. In addition, the ductility for the strengthened specimens C1 and C2 are about 29% and 59% greater than the control specimen C0, respectively.

Table 3. Yield force and displacement of the specimens C0, C1 and C2.

| Specimens | Drift (%) | Yield strength (kN) | Yield displacement ( $\Delta_y$ , mm) | Load capacity |
|-----------|-----------|---------------------|---------------------------------------|---------------|
| C0        | 1.00      | 250                 | 9.00                                  | 1.00          |
| C1        | 1.56      | 330                 | 14.00                                 | 1.32          |
| C2        | 1.44      | 400                 | 13.00                                 | 1.60          |

Table 4. Peak strength and displacement of the specimens C0, C1 and C2.

| Specimens | Drift (%) | Peak strength (kN) | Maximum displacement ( $\Delta_m$ , mm) | Load capacity | Ductility capacity |
|-----------|-----------|--------------------|---|---------------|--------------------|
| C0        | 2.00      | 320                | 20.00                                   | 1.00          | 2.22               |
| C1        | 3.25      | 498                | 40.00                                   | 1.55          | 2.86               |
| C2        | 4.00      | 573                | 46.00                                   | 1.79          | 3.54               |

#### 4.5. Strain Measurement of the Specimens

The relationships between the horizontal force and strain of the transverse and longitudinal reinforcements of the specimens C0, C1, C2 are presented in Figs. 10, 11, respectively. Those of the expanded metal reinforcements in the ferrocement of the strengthened specimens C1 and C2 are shown in Fig. 12.

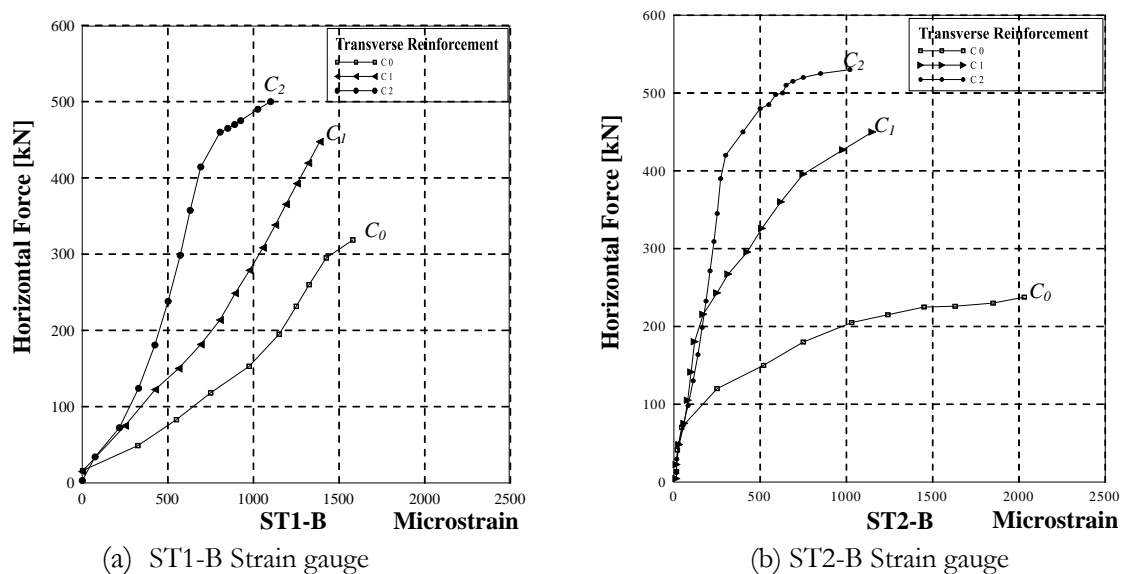


Fig. 10. Force and strain of the transverse reinforcements of the specimen C0, C1, C2.

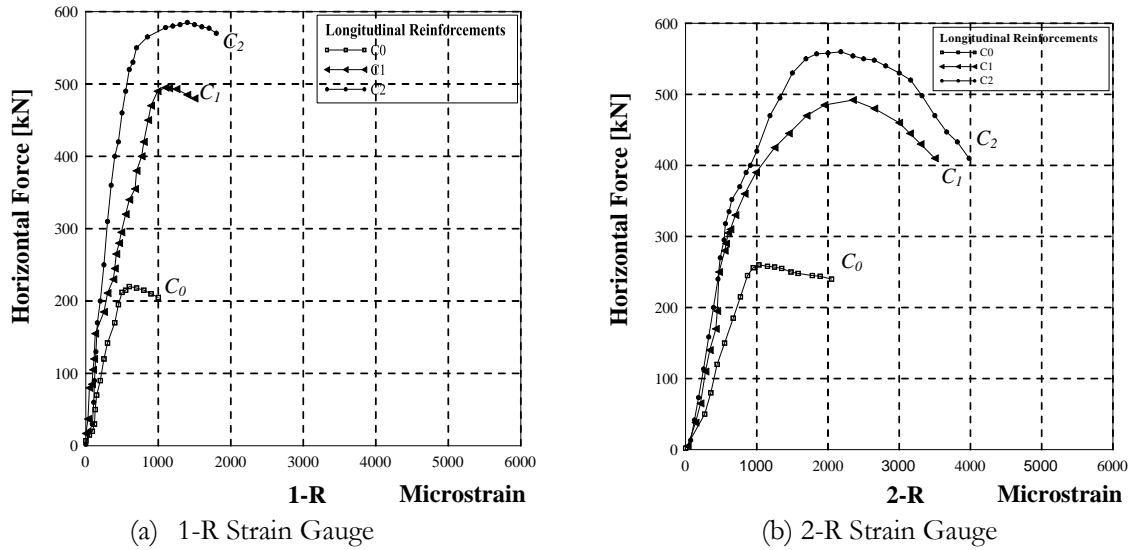


Fig. 11. Force and strain of the longitudinal reinforcements of the specimen C0,C1,C2.

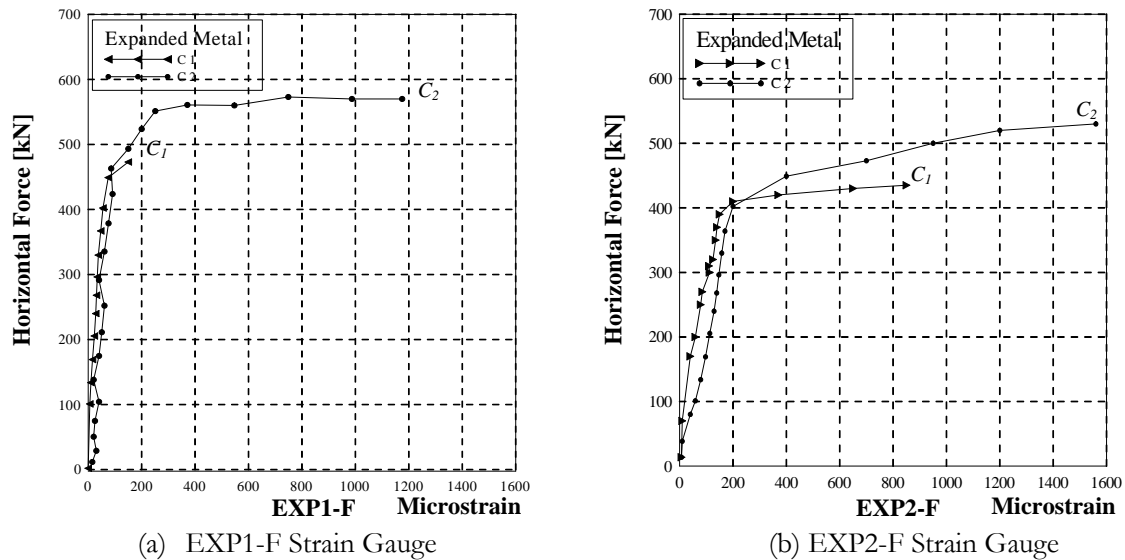


Fig. 12. Force and strain of the expanded metal reinforcement of the specimen C1, C2.

It can be observed that the strain of the reinforcement of all specimens increased in proportion to the applied horizontal force. The strains of the transverse reinforcement of the strengthened specimens C1, C2 were less than that of the control specimen C0. Meanwhile the strains of the longitudinal reinforcements of the strengthened specimens C1, C2 were larger than that of the control specimen C0. This indicated that the stirrups of the strengthened specimens carried less shear force than that of the control specimen. As a result, the shear mode of failure in the stirrup for the strengthened specimens was reduced and the flexure mode of the longitudinal reinforcement was dominant. The longitudinal reinforcement of the strengthened specimens C1 and C2 exhibited strain hardening behaviour and experienced large strain after yielding, as shown in Fig. 11b. This indicated that the premature failure of the column due to shear mode was shifted and the flexure mode was taken place. This behaviour is consistent with the failure mechanism of the strengthened specimens C1 and C2 which showed more flexural cracks rather than diagonal shear cracks indicating that the plastic hinge was formed. As a result, the strengthened columns became more ductile than the control column. The reduction of shear force in the stirrup was due to the effect of the expanded metal reinforcement which showed the increase of relatively large strain, particularly for the specimen C2, as shown in Fig. 12. The results showed that the effect of expanded metal improved the failure mode,

brittle shear mode of the strengthened specimens was shifted, and the ductile flexure mode became dominant, this is the desirable performance of the strengthened columns.

#### 4.6. Stiffness Degradation and Energy Dissipation

The stiffness degradation for the specimens C0, C1 and C2 are presented in Fig. 13a. It can be observed that the stiffness of all specimens was decrease with the increase of the drift levels due to the cumulative damage under each cyclic loading. The stiffness of the strengthened specimens was greater than that of the control specimen due to the presence of ferrocement. Among the strengthened column C1 and C2, the stiffness of the specimen C2 was approximately 20% greater than that of the specimen C1. Since the volume fraction of the specimen C2 was about two times that of the specimen C1, the increase of volume fraction of the expanded metal in the ferrocement significantly improved the stiffness of the strengthened column. The similar results can be observed for the energy dissipation, as shown in Fig. 13b. The amount of accumulated hysteretic energy of the strengthened columns was much greater than that of the original column. It is clear that the effect of volume fraction of the expanded metal in the ferrocement could enhance the energy dissipation capacity of the strengthened column.

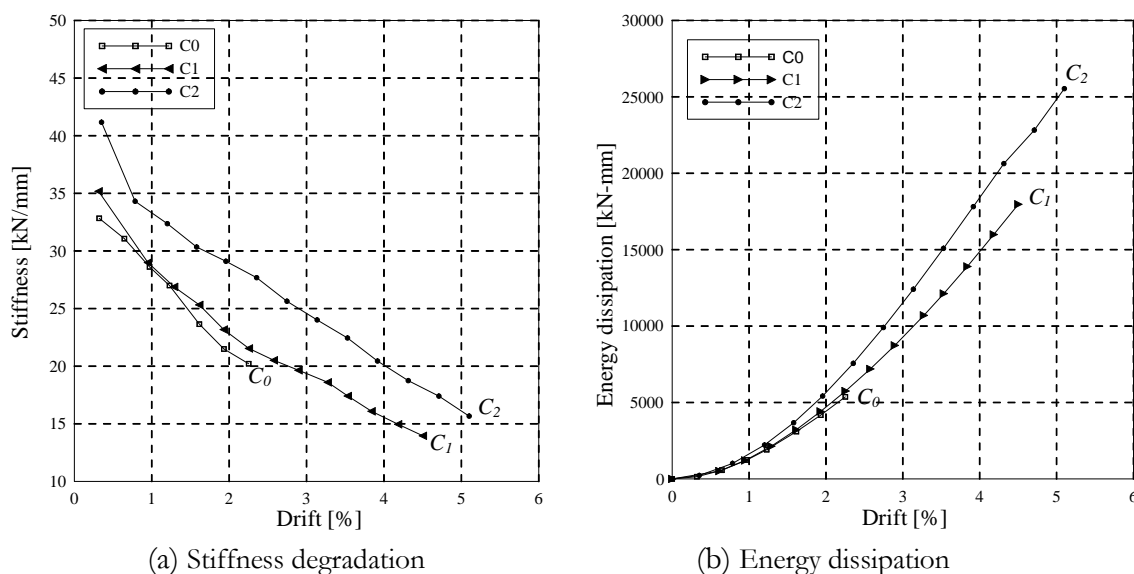


Fig. 13. Stiffness degradation and energy dissipation of the specimens C0, C1 and C2.

#### 4.7. Shear Strength of the Strengthened Column

To calculate the shear strength of the strengthened column, the following equations are proposed based on the suggestion of ACI 549.1R [10].

$$V_n = V_{n0} + V_{sf} \quad (1)$$

where,  $V_n$  is the nominal shear strength of the strengthened column which is the shear capacity of the strengthened column;

$V_{n0}$  is the nominal shear strength of the original column which may be calculated based on the modified Ohno-Arakawa's equation [27];

$V_{sf}$  is the shear strength of ferrocement which can be calculated as follows:

$$V_{sf} = \eta(nV_f tL_{sf}) \quad (2)$$

where  $V_f$  is the volume fraction of ferrocement reinforcement;

$\eta$  is the global efficiency factor for ferrocement reinforcement;

$n$  is the number of ferrocement jacket layers.

$t$  is the thickness of ferrocement jacket.  
 $L_s$  is the distance between the column base and the lateral load.  
 $f_y$  is the yield strength of ferrocement reinforcement.

The shear strength of ferrocement is calculated based on the shear strength of the effective area of reinforcement for mesh layer. When the effective area of reinforcement is multiplied by the global efficiency factor, it leads to the equivalent (effective) area of reinforcement in the loading direction considered. In general, the values of global efficiency factor were suggested by ACI 549.1R [10] for a member subjected to tension or bending. But there is no suggestion for shear due to the unavailable data on the shear capacity of ferrocement. From this study, the global efficiency factor  $\eta$  can be evaluated by using linear regression analysis of the relationship between shear strength of the tested specimens and the product of the parenthesis parameters ( $nV_f tL_s f_y$ ), as shown in Fig. 14. The slope of the representative straight line of 0.4614 is the global efficiency factor  $\eta$  for predicting the shear strength of the strengthened column using ferrocement with expanded metal. For design purpose, the global efficiency factor obtained from this study can be employed to predict the shear strength of the strengthened column using this type of ferrocement with expanded metal. It should be remarked that the global efficiency factor  $\eta$  obtained from this study was the pilot project for evaluating the shear strength of ferrocement with expanded metal. Further research study is required for an extensive experiment on the orientation, the size of the cells, and the number of cells of expanded metal reinforcement and the shape factors affecting on the shear strength of ferrocement.

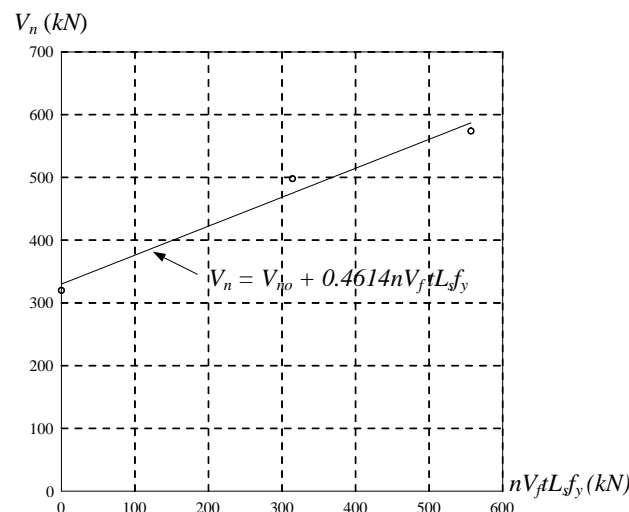


Fig. 14. Shear strength of the tested specimens and the parameters ( $nV_f tL_s f_y$ ).

## 5. Conclusions

An experimental study was carried out to investigate the seismic shear strength of reinforced concrete short columns strengthened with ferrocement and expanded metal. Based on the above results, the following conclusions can be drawn:

- The strengthened columns exhibited significant improvement of the shear strength, stiffness, displacement ductility, and hysteretic energy dissipation capacity when compared to the original column.
- The effect of ferrocement with expanded metal could control the crack width. It was observed that the crack width of the strengthened specimens were obviously smaller than the control specimen. In addition, the crack propagation was also improved. The expanded metal with small meshes provided the higher specific surface of reinforcement when compared to the large meshes. The interlocking between the small meshes and the mortar is better than the large mesh. As a result, the expanded metal

- mesh with the high specific surface provided the better performance for controlling the crack propagation.
- c) The effect of expanded metal could improve the shear mode of failure for the strengthened column. The brittle shear failure mode of the stirrup was reduced and the ductile flexure mode of the longitudinal reinforcement was dominant. The reduced shear force of the stirrup was compensated by the shear force of the expanded metal reinforcement which experienced relatively large strain.
  - d) At the end of testing, the expanded metal meshes were still interlocked with the corners of the strengthened columns and they maintained their original shape without twisting. This indicated that the technique of steel angle installation at the corners of column can successfully prevent the effect of sharpened corner wrapping of the mesh.
  - e) The global efficiency factor was proposed for evaluating the shear strength of ferrocement with expanded metal. More extensive experiments are required for further research study on the parameters that could affect the shear strength of ferrocement.

## Acknowledgement

This research is part of the research project “Research and Development for Strengthening of a Prototype School Building for Earthquake Resistant using Expanded Metal and Technology Transferring to a Case Study for School Building in Phan District Chiangrai Community Area”, supported by Biodiversity-based Economy Development Office (Public Organization), V & P Expanded Metal Co.Ltd. and Chulalongkorn University Research Funds.

## References

- [1] P. Lukkunaprasit, A. Ruangrassamee, T. Boonyatee, C. Chintanapakdee, K. Jankaew, N. Thanasisathit, and T. Chandrangu, “Performance of structures in the MW 6.1 Mae Lao earthquake in Thailand on May 5, 2014 and implications for future construction,” *Journal of Earthquake Engineering*, vol. 20, pp. 219-42, 2015.
- [2] K. Takiguchi and A. Abdullah, “Shear strengthening of reinforced concrete columns using ferrocement jacket,” *ACI Structural Journal*, vol. 98, no. 5, pp. 696–704, 2001.
- [3] P. R. Kumar, T. Oshima, S. Mikami, and T. Yamazaki, “Seismic retrofit of square reinforced concrete piers by ferrocement jacketing,” *Structure and Infrastructure Engineering*, vol. 1, no. 4, pp. 253–262, 2005.
- [4] A. Abdullah and K. Takiguchi, “An investigation into the behavior and strength of reinforced concrete columns strengthened with ferrocement jackets,” *Cement and Concrete Composites*, vol. 25, no. 2, pp. 233–242, 2003.
- [5] M. T. Kazemi and R. Morshed, “Seismic shear strengthening of R/C columns with ferrocement jacket,” *Cement and Concrete Composites*, vol. 27, pp. 834-842, 2005.
- [6] J. H. Choi, “Seismic retrofit of reinforced concrete circular columns using stainless steel wire mesh composite,” *Canadian Journal of Civil Engineering*, vol. 35, no. 2, pp. 140–147, 2008.
- [7] S. H. Kim and J. H. Choi, “Repair of earthquake damaged RC columns with stainless steel wire mesh composite,” *Advance Structural Engineering*, vol. 13, no. 2, pp. 393–401, 2010.
- [8] C. D. Johnston and S. G. Mattar, “Ferrocement behavior in tension and compression,” in *Proceedings, ASCE, ST5*, 1976, vol. 102, pp. 876-889.
- [9] M. E. Iorns and L. L. Watson, “Ferrocement boats reinforced with expanded metal,” *Journal of Ferrocement (Bangkok)*, vol. 7, no. 1, pp. 9-16, 1977.
- [10] ACI Committee, “Guide for the design, construction, and repair of ferrocement,” ACI 549.1R-93, American Concrete Institute, MI, USA, 1993.
- [11] C. Graciano, P. Teixeira, and G. Martinez, “Yielding shear resistance of expanded metal panels,” *Thin-Walled Structures*, vol. 138, pp. 286–292, 2019.
- [12] P. Teixeira, G. Martínez, and C. Graciano, “Shear response of expanded metal panels,” *Engineering Structures*, vol. 106, pp. 261–272, 2016.
- [13] Y. A. Al-Salloum “Influence of edge sharpness on the strength of square concrete columns confined with FRP composite laminates,” *Composites Part B: Engineering*, vol. 38, pp. 640–50, 2006.

- [14] L. Wang, “Effect of corner radius on the performance of CFRP-confined square concrete column,” M. Phil thesis, Department of Building and Construction, City University of Hong Kong, Hong Kong, 2007.
- [15] M. Soman and J. Mohan, “Rehabilitation of RC columns using ferrocement jacketing,” *Construction and Building Materials*, vol. 181, pp. 156–162, 2018.
- [16] A. B. M. A. Kaish, M. R. Alam, M. Jamil, M. F. M. Zain, and M. A. Wahed, “Improved ferrocement jacketing for restrengthening of square RC short column,” *Construction and Building Materials*, vol. 36, pp. 228–237, 2012.
- [17] A. B. M. A. Kaish, M. R. Alam, M. Jamil, and M. A. Wahed, “Ferrocement jacketing for restrengthening of square reinforced concrete column under concentric compressive load,” *Procedia Engineering*, vol. 54, pp. 720–728, 2013.
- [18] A. B. M. A. Kaish, M. Jamil, S. N. Raman, M. F. M. Zain, and M. R. Alam, “An approach to improve conventional square ferrocement jacket for strengthening application of short square RC column,” *Materials and Structures*, vol. 3, pp. 1025–1037, 2016.
- [19] B. Li, E. S. S. Lam, B. Wu, and Y. Y. Wang, “Experimental investigation on reinforced concrete interior beam-column joints rehabilitated by ferrocement jackets,” *Engineering Structures*, vol. 56, pp. 897–909, 2013.
- [20] B. Li, E. S. S. Lam, B. Wu, and Y. Y. Wang, “Seismic behavior of reinforced concrete exterior beam-column joints strengthened by ferrocement composites,” *Earthquakes and Structures*, vol. 9, no. 1, pp. 233–256, 2015.
- [21] B. Li and E. S. S. Lam, “Influence of interfacial characteristics on the shear bond behaviour between concrete and ferrocement,” *Construction and Building Materials*, vol. 176, pp. 462–469, 2018.
- [22] Japanese Standards Association, “Expanded metal standard by japanese industrial standard,” JIS Standard No. JIS G3351, 1987.
- [23] P. N. Dung and A. Plumier, “Behavior of expanded metal panels under shear loading,” in *Proceedings of SDSS RIO 2010 Stability and Ductility of Steel Structures Janeiro*, 2010, pp. 1101–1108.
- [24] P. N. Dung, “Seismically retrofitting reinforced concrete moment resisting frames by using expanded metal panels,” Doctoral Thesis, University of Liege, 2011.
- [25] American Society for Testing and Materials, “Standard test method for compressive strength of hydraulic-cement mortars,” ASTM Standard No. ASTM C349, 1977.
- [26] Federal Emergency Management Agency, “Interim testing protocol for determining the seismic performance characteristics of structural and nonstructural components,” Federal Emergency Management Agency, FEMA 461, Redwood City, 2007.
- [27] K. Sakino and Y. Sun, “Steel jacketing for improvement of column strength and ductility,” in *The 12th World Conference on Earthquake Engineering*, Auckland, New Zealand, 2000, pp. 2525–40.